HHS Public Access

Author manuscript

Obesity (Silver Spring). Author manuscript; available in PMC 2019 October 11.

Published in final edited form as:

Obesity (Silver Spring). 2019 May ; 27(5): 803–812. doi:10.1002/oby.22440.

Bile Diversion Improves Metabolic Phenotype Dependent on Farnesoid X Receptor (FXR)

Joseph F. Pierre[1,3,*], **Yuxin Li**[2,*], **Charles K. Gomes**[3], **Prahlad Rao**[3], **Eugene B. Chang**[1], **Deng Ping Yin**[2]

[1]Department of Medicine, the University of Chicago, Chicago, IL, USA.

[2]Department of Surgery,the University of Chicago, Chicago, IL, USA.

[3]Department of Pediatrics, University of Tennessee Health Science Center, Memphis, TN, USA.

Abstract

Objective.—The current study investigated whether bile diversion (BD) improves metabolic phenotype under farnesoid X receptor (FXR) deficiency.

Methods.—BD was performed in high-fat diet (HFD)-fed FXR knockout (FXRko) and wild-type (WT) animals. Metabolic phenotypes, circulating enteroendocrine hormones, total BAs and BA composition and cecal gut microbiota were analyzed.

Results.—FXR deficient mice are resistant to HFD-induced obesity; however, FXR deficient mice also develop hyperglycemia and exhibit increased liver weight, liver steatosis, and circulating triglycerides. BD increases circulating total BAs and taurine-b-muricholic acid (TbMCA), in line with normalized hyperglycemia and improved glucose tolerance in HFD-fed WT mice. FXR deficiency also increases total BA and TbMCA, but these animals remain hyperglycemic. While BD improved metabolic phenotype in HFD-FXRko mice, these improvements were not as effective as in WT mice. BD increased liver expression of FGF21 and PGC1ß and elevated circulating GLP-1 levels in WT mice, but not in FXRko mice. FXR deficiency altered gut microbiota composition with a specific increase in phylum Proteobacteria that may act as a possible microbial signature of some diseases. These cellular and molecular changes in FXRko mice may contribute to resistance towards improved metabolism.

Conclusions.—FXR signaling plays a pivotal role in improved metabolic phenotype following BD surgery.

Keywords

Bile acid receptors; bile diversion; obesity; FXR; mice

Corresponding authors: Deng Ping Yin, MD, PhD, Department of Surgery, SBRI J547/MC5026, University of Chicago, Chicago, IL 60637, Phone number: 773-702-5520, FAX number: 773-702-5518, dyin@surgery.bsd.uchicago.edu.

*J.F.P and Y.L. are co-first authors

Author Contribution: JFP and YL contributed to most *in vitro* and *in vivo* experiments; HY contributed to energy expenditure analysis; CG and PR contributed to bile acid analyses; EBC contributed to design the experiment, and DPY designed and wrote the manuscript. All authors approved the final version.

Conflicts of interest: All authors have declared that no conflict of interest exists.

Introduction

Mounting evidence suggests that the beneficial effects of bariatric surgery, such as Roux-en Y gastric bypass (RYGB) and vertical sleeve gastrectomy (VSG), may be associated with or induced by increases of circulating bile acids (BAs) (1–3). We previously demonstrated that delivery of BAs to the distal intestine using bile diversion (BD) surgery improves high-fat diet-induced obesity (DIO), insulin resistance and energy expenditure in wild type (WT) mice (4). The metabolic benefits induced by BD are associated with increased circulating BAs and with reconfiguration of the gut microbiota community structure (4).

BAs are dual-purpose molecules that serve digestive and hormone functions. From a hormone standpoint, they modulate glucose and lipid homeostasis acting through their receptors, the farnesoid X receptor (FXR) and G protein-coupled bile acid receptor 1 (TGR5) , which play an important role in maintaining glucose homeostasis (5–7). Activation of TGR5 promotes release of glucagon-like peptide-1 (GLP-1) that reduces gastrointestinal motility and exerts strong glucose-dependent insulinotropic and glucagonostatic actions on the pancreatic ß-cells (8–11). Activation of FXR reveals two contradictory characteristics: improving insulin release and sensitivity (12, 13) and promoting obesity and diabetes (14, 15). FXR activation stimulates glycogen synthesis, decreases gluconeogenesis and increases glycolysis, resulting in improved glucose tolerance and insulin sensitivity (13, 16, 17). FXR signaling also exerts strong insulinotropic actions on the pancreatic ß-cells and is considered a molecular mediator of the metabolic benefits of bariatric surgery (12, 18). A previous report shows that activation of FXR regulates TGR5 to release GLP-1 and serum GLP-1 levels are reduced in FXR deficient mice (19). However, FXR promotes the expression of ceramide that mediates a variety of cellular signaling events, resulting in enhanced mitochondrial permeability and inflammatory responses in the intestine. Accordingly, intestinal inhibition of FXR may reduce ceramides production and improve ß-cell function (20). In addition, the FXR antagonist taurine-b-muricholic acid (TbMCA) is effective in improving obesity associated metabolic parameters (21).

In the current study, we tested whether the global lack of FXR influences BD-induced metabolic alterations, including body weight and glucose homeostasis, enterohormones and adipokines, BA synthesis and microbiome composition. Accordingly, our data support the finding that FXR deficient mice are resistant to HFD-induced obesity. However, despite being leaner, mice lacking FXR display elevated blood glucose levels compared with WT on HFD. While BD surgery increases circulating total BAs and TbMCA, which induces metabolic benefit in WT mice, FXR deficient mice fail to respond to BD, despite elevated circulating total BAs and increased TbMCA both at baseline and following BD surgery when compared to WT. Our findings suggest that FXR is required for improved metabolic phenotype following BD surgery.

Materials and Methods

Mice and surgery

Age-matched FXR knockout (FXRko) mice and their wild-type littermate (WT) male mice purchased from Jackson Lab were used in the current study. Mice were fed a high-fat diet (HFD, fat calories 60%, Bio-Serv) or low-fat control diet (LFD, fat calories 11%, Bio-Serv). Four groups were designed, and 5 mice per group for LFD feeding and 10 mice per group for HFD feeding. After 8 weeks of diet feeding, 5 HFD-fed mice in each group underwent BD surgery and the other 5 mice used as controls. These mice were housed in the Animal Resources Center (ARC) at the University of Chicago in a specific pathogen-free, temperature-controlled and 12 hours light-dark cycle environment. The BD surgery was performed in HFD-fed mice under general anesthesia with isoflurane plus equal O_2 through a cone placed around the mouse's nose as described in previous reports (4, 22). In brief, these procedures require the anastomosis of the gallbladder to the distal jejunum at 10cm distance (BD) to the suspensory ligament of the duodenum. The surgical success rate was 100%, and there were no mice that died of the BD procedure. After the completion of surgery, mice had free access to HFD and water and were administered buprenorphine (0.1 mg/kg) and meloxicam (1.0 mg/kg) followed by meloxicam treatment (1.0 mg/kg) every 24 hours for 3 days. At 8 weeks following surgery (the end-point), tissues were collected under ketamine/xylazine anesthesia. All protocols were approved by Institutional Animal Care and Use Committee (IACUC) at the University of Chicago.

Analysis of metabolic phenotype

Blood glucose level was measured using a blood glucose meter (Accu-Chek Compact Plus, Roche Diabetes Care, Inc.). Oral gavage glucose tolerance tests (OGTT) were performed. Briefly, mice were fasted for 4 hours prior, and blood was sampled from the tail vein for glucose tests using the same glucose meter before and at 15, 30, 60, 90 and 120 min after oral gavage of dextrose (20%) at 2.0 mg/g body weight.

Body weight and diet consumption were analyzed every day up to the end-point. Metabolic analysis of energy balance was carried out using metabolic cages (TSE Systems, Chesterfield, MO) (23). Mice were placed individually in a TSE Labmaster System for 4 days, and food and water intake, physical activity, and O_2 uptake and CO_2 production were analyzed after a 2-day acclimation. The system was calibrated according to manufacturer's instructions prior to the start of the experiment.

Circulating ghrelin, GLP-1, GIP, Leptin, Resistin, and PAI-1 were analyzed, using a Bio-Plex Pro™ mouse diabetes immunoassay (Bio-Rad, Hercules, California) according to manufacturer's instructions.

Quantification Real-time RT-PCR (qRT-PCR) for mRNA analysis

The tissues were collected and immediately placed in Trizol reagent (Ambion, Austin, TX). Total RNA was obtained and was reverse-transcribed to complementary DNA (cDNA) using the Transcriptor First Strand cDNA Synthesis Kit (Roche, Indianapolis, IN), according to the manufacturer's instructions. RT-PCR amplification was consisted of an initial denaturation

step (95°C for 10 min), 45 cycles of denaturation (95°C for 10s), annealing (55°C for 20s) and extension (60°C for 30s), followed by a final incubation at 55°C for 30s and cooling at 40°C for 30s. All measurements were normalized by the expression of GAPDH gene that was considered as a stable housekeeping gene as described in our previous report (4).

Total BAs and BA composition analyses

Total BAs were quantified via enzymatic assay (Crystal Chem, Downers Grove, IL) in peripheral according to the manufacturer's instructions. BA compositions were analyzed as our previous report (4). Briefly, stock solutions of individual BAs and NDCA were prepared in methanol at a concentration of 5.0 μg/mL. Calibration standards were prepared by adding individual BAs at a concentration range of 12 ng/mL to 1.5 ug/mL Calibration standards were prepared by adding individual BAs at a concentration range of 12ng/mL to 1.5ug/mL to charcoal stripped human serum. 1.6μL of NDCA was added to 40μL of standards and samples. Deproteinization was carried out by adding 15X ice-cold methanol to 40μL of standards and samples. The samples were vortexed three times for 10 seconds each and stored at −20°C for 20 minutes. The supernatant was transferred to a new tube, evaporated under vacuum and dissolved in 100μL of 50% methanol. The tubes were centrifuged at 11,000xg for 1 min before transfer into specific vials for injection in to an LC-MS/MS system. Data were acquired on AB Sciex triple quadrupole mass spectrometer in negative ion mode coupled to Shimadzu Nexera XR HPLC system. Chromatographic separation was carried out on Thermo Scientific Accucore XLC8 column (4μm, 100 × 3mm I.D.). The oven temperature was set at 50°C. Separation was carried out over a gradient of 18 minutes with 28% B at 0 minutes to 90% B at 18 minutes. Quantitation of BAs was carried out on MultiQuant software v3.0.2 (AB Sciex).

Cecal content microbiota analysis

Gut microbiota in the cecal content was analyzed as described in our previous report (4). Briefly, primers specific for 16S rRNA V4-V5 region (Forward: 515F: 5'-GTGYCAGCMGCCGCGGTAA - 3' and Reverse: 806R: 5'-GGACTACHVGGGTWTCTAAT-3') that contained Illumina 3' adapter sequences, as well as a 12-bp barcode were used. Sequences were generated by an Illumina MiSeq DNA platform at Argonne National Laboratory and analyzed by the program Quantitative Insights Into Microbial Ecology (QIIME) (24). Operational Taxonomic Units (OTUs) were picked at 97% sequence identity using open reference OTU picking against the Greengenes database (25). Representative sequences were aligned via PyNAST, taxonomy assigned using the RDP Classifier, and a phylogenetic tree was built using FastTree.

Pathological examination

Selected naïve, HFD-fed and BD mice were sacrificed and the livers were collected for pathological examinations (H&E) at 8 weeks post-surgery. Significant lesions included steatosis, ballooning, and intraacinar and portal inflammation; and the lesions were graded as mild (1+, up to 33%), moderate (2+, 33–66%), and severe (3+, >66%).

***In vitro* and *in vivo* studies of activation of FXR signaling—**Inflammatory responses are mediated through inflammatory signaling pathways, such as NF-B, causing

TNFα expression. To test if the FXR agonist, chenodeoxycholic acid (CDCA), inhibited NF-B activity and TNFα expression in macrophages, bone marrow-derived macrophages (BMDMs) transfected with a luciferase gene under the control of the NF-B promoter were incubated with lipopolysaccharide (LPS, 0.025μg/ml), free-fatty acid (FFA, palmitic acid, 0.1μm) and CDCA (Sigma-Aldrich, 1.0μm). BMDMs were maintained in DMEM (Invitrogen) supplemented with 10% FCS at 37 ° C in a 5% CO2 incubator for 4 hours. NF-B activity was tested by luciferase assay (Promega) and TNFα by qRT-PCR. To test whether activation of FXR improves obesity and glucose tolerance, CDCD was administered to HFD-fed WT mice at a dose of 150mg/kg (dissolved in 100μl 1% carboxymethylcellulose or CMC) by oral gavage daily for 4 weeks. The same dose of lithocholic acid (LCA) was administered to HFD-fed WT mice by oral gavage daily for 4 weeks (26).

Statistical analysis

Sequence reads were analyzed using QIIME software. Significant changes in OTU abundance were assessed using Kruskal Wallis test (FDR correction $p \leq 0.05$). Differences between groups in microbiota phylum and genus levels were analyzed by Kruskal-Wallis. All other comparisons were calculated using ANOVA tests (StatView 4.5, Abacus Concepts, Berkeley, CA) and $p < 0.05$ was considered significant. The results are presented as mean ± SEM.

Results

BD improves body weight and glucose tolerance in FXRko mice, but not as effectively as in WT mice.

The current study examined whether BD surgery improves obesity and glucose tolerance in the absence of FXR compared to WT mice. Figure 1 showed no statistical differences in body weight between LFD-fed WT and LFD-fed FXRko animals ($p > 0.05$, Figure 1A, body weight in grams and Figure 1B, body weight in percentage). However, HFD-fed FXRko mice displayed significantly lower body weight at 8 weeks on HFD feeding compared to HFD-fed WT mice (FXRko vs. WT, $p < 0.05$, Figures 1A-1B), suggesting that mice lacking FXR are resistant to HFD-induced obesity. These findings set the stage to determine whether FXR mediated the metabolic benefits induced by BD in age-matched WT and FXRko mice fed HFD for 8 weeks. We observed that BD significantly improved body weight (Figure 1C, body weight in grams and Figure 1D, body weight in percentage) and fat mass (epididymal white adipose tissue or eWAT, Figure 1E and Figure 1F) in HFD-fed WT and FXRko animals. Liver weight from age-matched LFD-fed FXRko mice exhibited marked increase, compared to WT mice; however, absolute liver weight (in gram) was not significantly changed in HFD-fed FXRko mice due to resistance to DIO (Figure 1G). The ratio of liver/body weight was elevated in LFD-fed and BD-treated FXRko mice as compared to WT mice (Figure 1H).

Blood glucose and oral glucose tolerance test (OGTT) were measured in WT and FXRko mice after fasting 4 hours. Fasting blood glucose levels were significantly increased in age-matched FXRko mice following 8 weeks of LFD or HFD feeding compared to WT animals (FXRko-LFD vs. WT-LFD, $p < 0.001$; FXRko-HFD vs. WT-HFD, $p = 0.05$, Figure 2A).

However, there were no differences in response to OGTT across groups (Figures 2B-2C). The current data suggest that mice lacking FXR develop chronic hyperglycemia and maintain normal glucose tolerance. BD improved HFD-induced hyperglycemia in HFD-fed WT and HFD-fed FXRko mice; however, blood glucose maintained at higher levels in FXRko mice (≈ 200mg/dL, Figure 2D). BD resulted in a better outcome in improving glucose tolerance in HFD-fed WT mice than in HFD-fed FXRko mice (WT-BD vs. FXRko-BD, $p = 0.004$, Figures 2E-2F). These findings collectively show that BD does not significantly improve hyperglycemia and glucose tolerance in the absence of FXR.

FXR is required for hepatic responses after BD surgery

Mice lacking FXR revealed enlarged liver (Figure 1F), liver steatosis with moderate (LFD-fed) and severe (HFD-fed) structural damage (Figure 3A) and increased circulating triglycerides in LFD-fed FXRko mice (Figure 3B), consistent with previous findings linking FXRko and lipid dysregulation (27). While HFD-fed WT mice were characterized by the accumulation of lipid droplets, HFD-fed FXRko livers displayed many micro lipid droplets (Figure 3A). Following BD, liver steatosis improved in HFD-fed WT mice, but was largely unchanged in FXRko animals, where the abundance of small lipid vesicles was visible in all samples. Fibroblast growth factor 21 (FGF21), a member of the fibroblast growth factor family of signaling molecules, plays an important role in protecting against obesity-induced hepatic metabolic stress by enhancing fatty acid oxidation and tricarboxylic acid cycle flux. The pathogenesis of liver steatosis and non-alcoholic fatty liver disease (NAFLD) involves dysregulation of peroxisome proliferation-activated receptor-α (PPARα) and FGF21 (28). Our prior work demonstrated that increased primary BAs following BD promoted expression of FGF21, PPARα and peroxisome proliferator-activated receptor γ coactivator-1ß (PGC1ß) in the liver of HFD-fed WT mice (4). Consistently, this study found that BD significantly increased hepatic FGF21 gene expression in HFD-fed WT mice; however, this was not observed in FXRko mice (Figure 3C). PGC-1ß is a nuclear receptor that regulates fatty acid oxidation and protects against liver steatosis (29). PGC-1ß also mediates diet-induced changes in FGF21 gene expression, where FGF21 induces and activates PPARα to liver steatosis (30). HFD reduced expression of PGC-1ß in WT and FXRko mice. BD significantly increased PGC-1ß expression in the livers of WT mice, but BD failed to promote PGC-1ß in FXRko animals (Figure 3D). Interestingly, PPARα expression was elevated in LFD-fed and HFD-fed FXRko mice, but decreased following BD surgery in these animals. In contrast, BD promoted PPARα expression in WT mice compared to baseline levels observed under LFD and HFD feeding (Figure 3E).

The lack of FXR alters expression of endocrine hormones and adipokines

BD promoted increase in serum GLP-1 in WT animals (WT-BD vs. WT-LFD and WT-HFD, $p < 0.0001$, Figure 4A), consistent with previous work (4). Although BD increased the average level of GLP-1 in HFD-fed FXRko mice, GLP-1 level in WT mice was significantly higher than FXRko mice ($p < 0.05$, Figure 4A). HFD promoted leptin expression, which is associated with increased fat mass, and BD reduced leptin production in HFD-fed WT mice. However, leptin was not significantly increased in HFD-fed FXRko mice (Figure 4B), indicating a resistance to DIO. HFD elevated resistin, and BD reduced resistin, but this was not statistically significant ($p > 0.05$, Figure 4C). We observed reduced ghrelin levels in

HFD-fed WT and HFD-fed FXRko mice, and while BD reversed this, this was not significant ($p > 0.05$, Figure 4D). Finally, there were no differences in GIP and PAI-1 across all groups ($p > 0.05$, Figures 4E-4F).

The lack of FXR alters BA and gut microbiota homeostasis

To test whether the lack of FXR alters BA synthesis and composition, we analyzed circulating total BAs and BA composition. Total BAs were increased in LFD-fed mice (FXRko-LFD vs. WT-LFD, $p < 0.01$) and BD-treated FXRko mice (FXRko-BD vs. WT-BD, $p < 0.01$). TbMCA was increased in HFD-fed FXRko mice (FXR-HFD vs. WT-HFD, $p < 0.05$) and BD-treated WT mice (WT-BD vs. WT-HFD, $p < 0.01$) (Supporting information Figures S1A-S1B).

To examine whether FXRko influences gut microbiota composition, cecal contents were collected for next generation sequencing, targeting the 16S rRNA V4-V5 region at 8 weeks post-surgery. Unweighted analysis distinguishes differences in rare taxa, since absolute abundance is ignored. This analysis suggests these treatment conditions select for distinct microbial community membership. Figure 5A demonstrates that LFD-fed FXRko mice cluster distinctly from LFD-fed WT mice (left upper panels), and HFD-fed FXRko and BD-treated FXRko mice cluster distinctly from WT mice (right upper and right lower panels). Shannon diversity analysis showed decreased diversity in HFD-fed WT and FXRko mice and BD-treated WT mice, but not in BD-treated FXRko mice (Figure 5B). The Phyla Firmicutes and Bacteroidetes showed differences across LFD-fed and HFD-fed WT and FXRko animals (Figure 5C,5D,5F&5G). Interestingly, Proteobacteria was significantly increased in LFD-, HFD- and BD-treated FXRko mice (Figures 5E,5H&5K). At the genus level, the lack of FXR decreased *Bacteroides* (in LFD- and HFD-fed FXRko mice) and *Lactobacillus* (in LFD-fed and BD-treated FXRko mice) and increased *Desulfovibrionaceae* in all LFD- and HFD-fed and BD-treated FXRko animals (Supporting information Figure S2).

To test whether the lack of FXR influences BA conversion, we analyzed predictive gene orthologues from the 16S data for bacterial-derived BSH and 7α-HSDH. The results showed decrease of BSH abundance in LFD-fed and BD-treated FXRko mice (Supporting information Figure S3A). In contrast, 7α-HSDH abundance was significantly increased in LFD-fed, HFD-fed and BD-treated FXRko mice (Supporting information Figure S3B).

Activation of FXR inhibits inflammatory reaction and improves glucose tolerance

Activation of FXR has been shown to inhibit inflammatory reactions (31, 32). We tested whether the FXR agonist, CDCA, attenuates inflammatory response and improves metabolic phenotype. In the BMDM culture, FFA, increased luciferase activity, indicating increased NF-B activity, which was inhibited by additional CDCA (Figure 6A). TNFα mRNA was elevated by the stimulation of FFA but also inhibited by CDCA (Figure 6B). The results showed that the treatment with CDCA, but not LCA or vehicle, improved glucose tolerance (Figures 6C-6D).

Discussion

The beneficial effects of bariatric surgery, such as RYGB and VSG, may be associated with delivery of BAs to the distal intestine and increases of circulating BAs that trigger downstream signaling pathway via the activation of BA receptors (1–3). Consistent with our previous report (4), current findings demonstrate that delivery of BAs to the distal intestine by BD improves metabolic phenotype in HFD-fed WT mice. Mice lacking FXR diverge from WT mice with two contradictory characteristics: resistance to HFD-induced obesity associated with increased PPARα and the development of hyperglycemia along with increased circulating total BAs and TbMCA. Previous findings demonstrated that the absence of FXR reduces the ability of VSG to improve body weight and glucose tolerance (12). The current study shows that BD improves hyperglycemia, glucose tolerance and liver steatosis in HFD-fed WT mice in concert with significant increases of circulating GLP-1 levels and liver FGF21 gene expression in HFD-fed WT mice. However, while BD surgery improves hyperglycemia and glucose tolerance in HFD-fed FXRko mice. These improvements were not as marked compared to HFD-fed WT mice, suggesting FXR in part mediates metabolic benefits of BD.

BAs are synthesized from cholesterol in the liver, and the rate-limiting enzyme CYP7A1 initiates the classic pathway of BA synthesis, which is regulated by FXR. The absence of FXR increases BA synthesis characterized by increased circulating primary BAs, including TbMCA. BD delivers BAs to the distal intestine where increased TbMCA inhibits FXR and may contribute to improved metabolic phenotype, including reduced body weight, fat mass and energy expenditure (33). However, increased TbMCA does not improve hyperglycemia and glucose tolerance in HFD-fed FXRko mice, indicating dependency on FXR signaling. Hepatic deficiency of FXR contributes to lipid accumulation in the liver (34), whereas impaired FXR signaling in ß-cells influences insulin release (35). Previous reports suggest that activation of FXR inhibits or promotes GLP-1 secretion (19, 36). Our results show that while BD results in increases in circulating GLP-1 in both HFD-fed WT mice and HFD-fed FXRko mice, GLP-1 levels were significantly higher in WT mice than FXRko mice consistent with previous findings that FXR may work in concert with TGR5 in promoting GLP-1 secretion (19). Reduced GLP-1 secretion may also contribute to reduced metabolic response in global FXR deficiency following BD surgery.

In the intestine, BAs and the microbiota reciprocally control their compositional profile. HFD induces increased phylum Fimicutes or Fimicutes/Bacteroidetes ratio, whereas BD surgery enhances Bacteroidetes in WT mice (4). Recent findings have shown that FXR activation alters gut microbiota composition in humans (37). The current data show distinct distribution of cecal microbiome in LFD- and HFD-fed FXRko mice with decrease of phylum Bacteroidetes. Within Bateroidetes, the relative abundance of *Bacteroides* was decreased in LFD-fed and HFD-fed FXRko mice. More interestingly, the lack of FXR led to an increase in the phylum Proteobacteria that produce lipopolysaccharide (LPS) and act as a possible microbial signature of diseases, including metabolic disorders (38). Within the phylum Proteobacteria, the relative abundance of the gram-negative bacteria family *Desulfovibrionaceae* was increased in FXR animals, which may contribute to intestinal inflammation (39). BAs are deconjugated by bacterial-derived BSH as the first step in the

generation of secondary BAs. Subsequently, the action of bacterial 7α-hydroxysteroid dehydrogenases (7α-HSDH) on deconjugation results in the production of secondary BAs (40). Our findings show that the lack of FXR resulted in a reduction of *Bacteroides*-derived BSH and an increase in 7α-HSDH that catalyzes the bioconversion of CA and CDCA to 7-oxo-DCA and 7-oxo-LCA, respectively consistent with a previous report (18). 7α-HSDH are widespread among members of Firmicutes-derived genera *Clostridium*, *Eubacterium*, *Bacteroides* or *Escherichia* (41, 42).

FXR agonists have been utilized as therapy for obesity and diabetes in rodents (43) and in humans (44). However, a previous report indicates that FXR agonists decrease energy expenditure and induce obesity and insulin resistance in mice (15). Our data shows that FXR agonist CDCA inhibits FFA-induced NF-KB activity and TNFα expression *in vitro* and improves glucose tolerance *in vivo*. One major limitation of our findings relates the evidence that human and mouse BA composition are markedly different, i.e. primary BAs in humans include cholic acid (CA) and CDCA conjugated with glycine, whereas mice also produce MCA species conjugated with taurine (TaMCA and TbMCA). CDCA is an FXR agonist, whereas TbMCA is an FXR antagonist (45). Consequently, the extrapolation of BA related results in mice must be carefully interpreted concerning human implications. Another limitation of this study is that using global knockout of FXR cannot differentiate the tissue specific effects of FXR activity or modulation. However, taken together this work demonstrates an important role for FXR in the regulation of BA homeostasis, energy balance, and glucose metabolism.

In conclusion, these findings demonstrate that mice lacking FXR are resistant to HFD-induced obesity associated with increased PPARα. However, the absence of FXR also leads to hyperglycemia and dysregulation of BA and microbiota homeostasis. While BD improves body weight and glucose tolerance in FXRko mice, it is not as effective compared with WT mice. Finally, the FXR agonist CDCA inhibits FFA-mediated NF-KB activity and TNFα expression *in vitro* and improves glucose tolerance in HFD-fed WT mice. Our results contribute to the understanding of the mixed metabolic phenotypes observed in global FXR knockouts and provide the potential to develop tissue specific FXR manipulations for the treatment of obesity and type 2 diabetes.

Supplementary Material

Refer to Web version on PubMed Central for supplementary material.

Acknowledgments

Fund Statement: This work was supported in part by the CTSA grant (CTSA TR000430) to DPY, NIH grants P30DK42086 (DDRCC) and DK097268 to EBC and NIH grant DK020595 to the Metabolic Core at the University of Chicago.

References

1. Schauer PR, Bhatt DL, Kirwan JP, Wolski K, Brethauer SA, Navaneethan SD, et al. Bariatric surgery versus intensive medical therapy for diabetes−−3-year outcomes. The New England journal of medicine 2014;370(21):2002–13. [PubMed: 24679060]

2. Thoni V, Pfister A, Melmer A, Enrich B, Salzmann K, Kaser S, et al. Dynamics of Bile Acid Profiles, GLP-1, and FGF19 After Laparoscopic Gastric Banding. The Journal of clinical endocrinology and metabolism 2017;102(8):2974–84. [PubMed: 28591793]

3. Kohli R, Bradley D, Setchell KD, Eagon JC, Abumrad N, Klein S. Weight loss induced by Roux-en-Y gastric bypass but not laparoscopic adjustable gastric banding increases circulating bile acids. The Journal of clinical endocrinology and metabolism 2013;98(4):E708–12. [PubMed: 23457410]

4. Pierre JF, Martinez KB, Ye H, Nadimpalli A, Morton TC, Yang J, et al. Activation of bile acid signaling improves metabolic phenotypes in high-fat diet-induced obese mice. American journal of physiology Gastrointestinal and liver physiology 2016;311(2):G286–304. [PubMed: 27340128]

5. Simonen M, Dali-Youcef N, Kaminska D, Venesmaa S, Kakela P, Paakkonen M, et al. Conjugated bile acids associate with altered rates of glucose and lipid oxidation after Roux-en-Y gastric bypass. Obesity surgery 2012;22(9):1473–80. [PubMed: 22638681]

6. Patti ME, Houten SM, Bianco AC, Bernier R, Larsen PR, Holst JJ, et al. Serum bile acids are higher in humans with prior gastric bypass: potential contribution to improved glucose and lipid metabolism. Obesity 2009;17(9):1671–7. [PubMed: 19360006]

7. Ahmad NN, Pfalzer A, Kaplan LM. Roux-en-Y gastric bypass normalizes the blunted postprandial bile acid excursion associated with obesity. International journal of obesity 2013;37(12):1553–9. [PubMed: 23567924]

8. Manning S, Batterham RL. The role of gut hormone peptide YY in energy and glucose homeostasis: twelve years on. Annual review of physiology 2014;76:585–608.

9. Nannipieri M, Baldi S, Mari A, Colligiani D, Guarino D, Camastra S, et al. Roux-en-Y gastric bypass and sleeve gastrectomy: mechanisms of diabetes remission and role of gut hormones. The Journal of clinical endocrinology and metabolism 2013;98(11):4391–9. [PubMed: 24057293]

10. Bose M, Machineni S, Olivan B, Teixeira J, McGinty JJ, Bawa B, et al. Superior appetite hormone profile after equivalent weight loss by gastric bypass compared to gastric banding. Obesity 2010;18(6):1085–91. [PubMed: 20057364]

11. Shin ED, Estall JL, Izzo A, Drucker DJ, Brubaker PL. Mucosal adaptation to enteral nutrients is dependent on the physiologic actions of glucagon-like peptide-2 in mice. Gastroenterology 2005;128(5):1340–53. [PubMed: 15887116]

12. Ryan KK, Tremaroli V, Clemmensen C, Kovatcheva-Datchary P, Myronovych A, Karns R, et al. FXR is a molecular target for the effects of vertical sleeve gastrectomy. Nature 2014;509(7499):183–8. [PubMed: 24670636]

13. Zhang Y, Lee FY, Barrera G, Lee H, Vales C, Gonzalez FJ, et al. Activation of the nuclear receptor FXR improves hyperglycemia and hyperlipidemia in diabetic mice. Proceedings of the National Academy of Sciences of the United States of America 2006;103(4):1006–11. [PubMed: 16410358]

14. Prawitt J, Abdelkarim M, Stroeve JH, Popescu I, Duez H, Velagapudi VR, et al. Farnesoid X receptor deficiency improves glucose homeostasis in mouse models of obesity. Diabetes 2011;60(7):1861–71. [PubMed: 21593203]

15. Watanabe M, Horai Y, Houten SM, Morimoto K, Sugizaki T, Arita E, et al. Lowering bile acid pool size with a synthetic farnesoid X receptor (FXR) agonist induces obesity and diabetes through reduced energy expenditure. The Journal of biological chemistry 2011;286(30):26913–20. [PubMed: 21632533]

16. Cipriani S, Mencarelli A, Palladino G, Fiorucci S. FXR activation reverses insulin resistance and lipid abnormalities and protects against liver steatosis in Zucker (fa/fa) obese rats. Journal of lipid research 2010;51(4):771–84. [PubMed: 19783811]

17. Ma K, Saha PK, Chan L, Moore DD. Farnesoid X receptor is essential for normal glucose homeostasis. The Journal of clinical investigation 2006;116(4):1102–9. [PubMed: 16557297]

18. Gonzalez FJ, Jiang C, Patterson AD. An Intestinal Microbiota-Farnesoid X Receptor Axis Modulates Metabolic Disease. Gastroenterology 2016;151(5):845–59. [PubMed: 27639801]

19. Pathak P, Liu H, Boehme S, Xie C, Krausz KW, Gonzalez F, et al. Farnesoid X receptor induces Takeda G-protein receptor 5 Crosstalk to regulate Bile Acid Synthesis and Hepatic Metabolism. The Journal of biological chemistry 2017.

20. Chavez JA, Siddique MM, Wang ST, Ching J, Shayman JA, Summers SA. Ceramides and glucosylceramides are independent antagonists of insulin signaling. The Journal of biological chemistry 2014;289(2):723–34. [PubMed: 24214972]
21. Jiang C, Xie C, Lv Y, Li J, Krausz KW, Shi J, et al. Intestine-selective farnesoid X receptor inhibition improves obesity-related metabolic dysfunction. Nature communications 2015;6:10166.
22. Flynn CR, Albaugh VL, Cai S, Cheung-Flynn J, Williams PE, Brucker RM, et al. Bile diversion to the distal small intestine has comparable metabolic benefits to bariatric surgery. Nature communications 2015;6:7715.
23. Asayama K, Okada Y, Kato K. Peroxisomal beta-oxidation in liver and muscles of gold-thioglucose-induced obese mice: correlation with body weight. Int J Obes 1991;15(1):45–9.
24. Caporaso JG, Kuczynski J, Stombaugh J, Bittinger K, Bushman FD, Costello EK, et al. QIIME allows analysis of high-throughput community sequencing data. Nat Methods 2010;7(5):335–6. [PubMed: 20383131]
25. Lee CK, Herbold CW, Polson SW, Wommack KE, Williamson SJ, McDonald IR, et al. Groundtruthing next-gen sequencing for microbial ecology-biases and errors in community structure estimates from PCR amplicon pyrosequencing. PloS one 2012;7(9):e44224. [PubMed: 22970184]
26. Parks DJ, Blanchard SG, Bledsoe RK, Chandra G, Consler TG, Kliewer SA, et al. Bile acids: natural ligands for an orphan nuclear receptor. Science 1999;284(5418):1365–8. [PubMed: 10334993]
27. Sinal CJ, Tohkin M, Miyata M, Ward JM, Lambert G, Gonzalez FJ. Targeted disruption of the nuclear receptor FXR/BAR impairs bile acid and lipid homeostasis. Cell 2000;102(6):731–44. [PubMed: 11030617]
28. Montagner A, Polizzi A, Fouche E, Ducheix S, Lippi Y, Lasserre F, et al. Liver PPARalpha is crucial for whole-body fatty acid homeostasis and is protective against NAFLD. Gut 2016;65(7): 1202–14. [PubMed: 26838599]
29. Goncalves D, Barataud A, De Vadder F, Vinera J, Zitoun C, Duchampt A, et al. Bile Routing Modification Reproduces Key Features of Gastric Bypass in Rat. Annals of surgery 2015.
30. Mottillo EP, Bloch AE, Leff T, Granneman JG. Lipolytic products activate peroxisome proliferator-activated receptor (PPAR) alpha and delta in brown adipocytes to match fatty acid oxidation with supply. The Journal of biological chemistry 2012;287(30):25038–48. [PubMed: 22685301]
31. Bijsmans IT, Guercini C, Ramos Pittol JM, Omta W, Milona A, Lelieveld D, et al. The glucocorticoid mometasone furoate is a novel FXR ligand that decreases inflammatory but not metabolic gene expression. Scientific reports 2015;5:14086. [PubMed: 26369990]
32. Hao H, Cao L, Jiang C, Che Y, Zhang S, Takahashi S, et al. Farnesoid X Receptor Regulation of the NLRP3 Inflammasome Underlies Cholestasis-Associated Sepsis. Cell metabolism 2017;25(4): 856–67 [PubMed: 28380377]
33. Li F, Jiang C, Krausz KW, Li Y, Albert I, Hao H, et al. Microbiome remodelling leads to inhibition of intestinal farnesoid X receptor signalling and decreased obesity. Nature communications 2013;4:2384.
34. Schmitt J, Kong B, Stieger B, Tschopp O, Schultze SM, Rau M, et al. Protective effects of farnesoid X receptor (FXR) on hepatic lipid accumulation are mediated by hepatic FXR and independent of intestinal FGF15 signal. Liver international : official journal of the International Association for the Study of the Liver 2015;35(4):1133–44. [PubMed: 25156247]
35. Schittenhelm B, Wagner R, Kahny V, Peter A, Krippeit-Drews P, Dufer M, et al. Role of FXR in beta-cells of lean and obese mice. Endocrinology 2015;156(4):1263–71. [PubMed: 25599407]
36. Trabelsi MS, Daoudi M, Prawitt J, Ducastel S, Touche V, Sayin SI, et al. Farnesoid X receptor inhibits glucagon-like peptide-1 production by enteroendocrine L cells. Nature communications 2015;6:7629.
37. Friedman ES, Li Y, Shen TD, Jiang J, Chau L, Adorini L, et al. FXR-Dependent Modulation of the Human Small Intestinal Microbiome by the Bile Acid Derivative Obeticholic Acid. Gastroenterology 2018.

38. Carvalho FA, Koren O, Goodrich JK, Johansson ME, Nalbantoglu I, Aitken JD, et al. Transient inability to manage proteobacteria promotes chronic gut inflammation in TLR5-deficient mice. Cell host & microbe 2012;12(2):139–52. [PubMed: 22863420]

39. Nagata N, Xu L, Kohno S, Ushida Y, Aoki Y, Umeda R, et al. Glucoraphanin Ameliorates Obesity and Insulin Resistance Through Adipose Tissue Browning and Reduction of Metabolic Endotoxemia in Mice. Diabetes 2017;66(5):1222–36. [PubMed: 28209760]

40. Labbe A, Ganopolsky JG, Martoni CJ, Prakash S, Jones ML. Bacterial bile metabolising gene abundance in Crohn's, ulcerative colitis and type 2 diabetes metagenomes. PloS one 2014;9(12):e115175. [PubMed: 25517115]

41. Gerard P Metabolism of cholesterol and bile acids by the gut microbiota. Pathogens 2013;3(1):14–24. [PubMed: 25437605]

42. Fukiya S, Arata M, Kawashima H, Yoshida D, Kaneko M, Minamida K, et al. Conversion of cholic acid and chenodeoxycholic acid into their 7-oxo derivatives by Bacteroides intestinalis AM-1 isolated from human feces. FEMS microbiology letters 2009;293(2):263–70. [PubMed: 19243441]

43. Ma Y, Huang Y, Yan L, Gao M, Liu D. Synthetic FXR agonist GW4064 prevents diet-induced hepatic steatosis and insulin resistance. Pharmaceutical research 2013;30(5):1447–57. [PubMed: 23371517]

44. Mudaliar S, Henry RR, Sanyal AJ, Morrow L, Marschall HU, Kipnes M, et al. Efficacy and safety of the farnesoid X receptor agonist obeticholic acid in patients with type 2 diabetes and nonalcoholic fatty liver disease. Gastroenterology 2013;145(3):574–82 [PubMed: 23727264]

45. Sayin SI, Wahlstrom A, Felin J, Jantti S, Marschall HU, Bamberg K, et al. Gut microbiota regulates bile acid metabolism by reducing the levels of tauro-beta-muricholic acid, a naturally occurring FXR antagonist. Cell metabolism 2013;17(2):225–35. [PubMed: 23395169]

Short bullet-points:

What is already known about this subject?

The beneficial effects of bariatric surgery may be associated with increased circulating bile acids. Specifically, delivery of bile acids to the distal intestine by the bile diversion (BD) and other bile diverting procedures enhances bile acid signaling and improves obesity and insulin resistance.

Increased bile acids in the distal gut activate bile acid receptor FXR, which exhibits the dual characteristics of improving insulin sensitivity but also worsening diabetes. However, whether the lack of FXR influences BD-induced metabolic alterations remains unknown.

What does this study add?

BD surgery completely diverts bile acids to the distal jejunum and improves obesity and glucose tolerance associated with the modulation of bile acid and gut microbiota homeostasis. However, a deficiency of FXR may decrease the metabolic benefits associated with BD surgery due to the dysregulation of bile acid synthesis, gut microbiota composition and enterohormones release. Thus, FXR signaling may play a critical role in improving the metabolic phenotype observed with BD surgery.

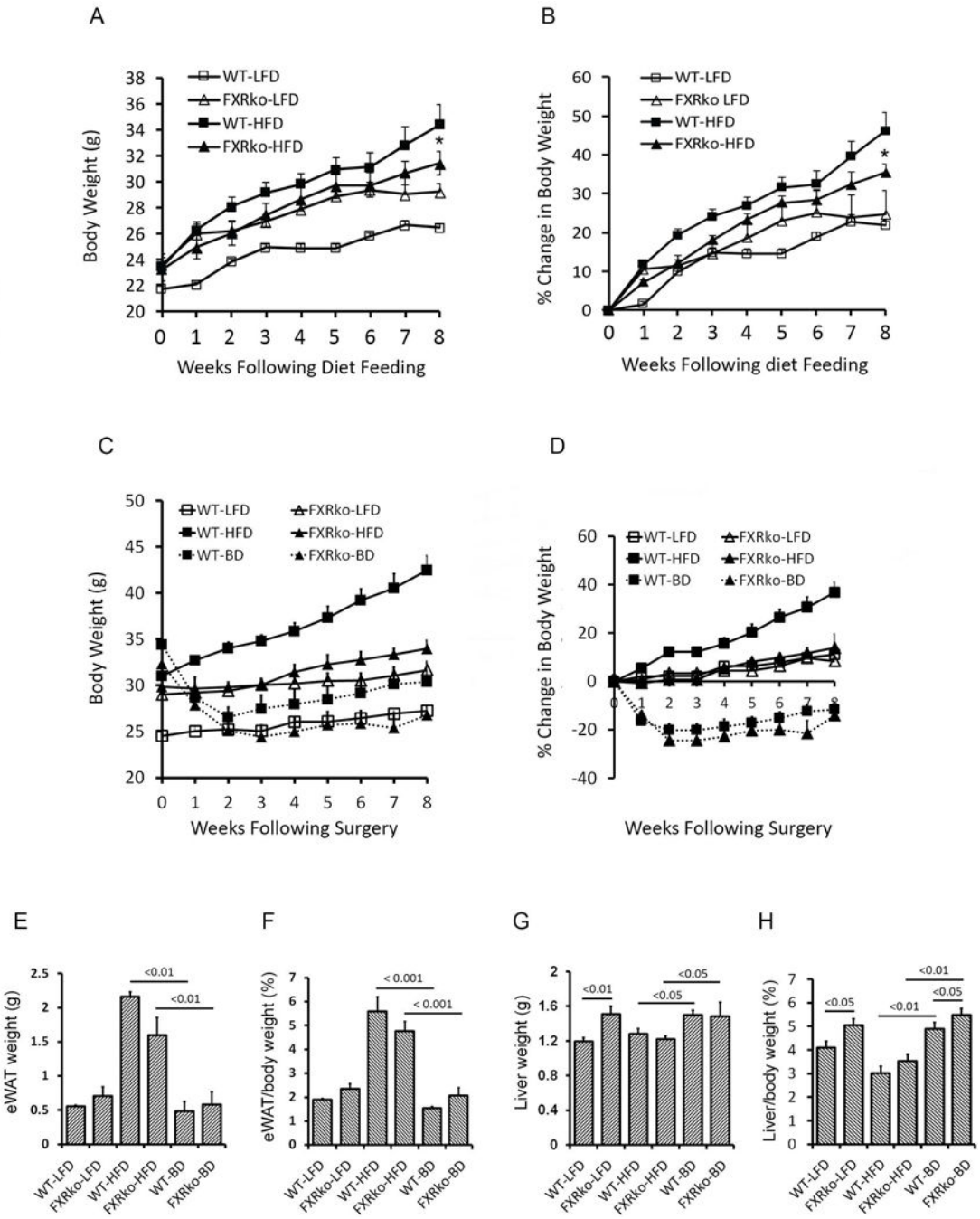

Figure 1.

Animals lacking FXR are resistant to DIO but liver weight is increased. (A) Body weight changes in grams in LFD-fed (n = 5 each group) and HFD-fed (n = 10 each group) WT and FXRko mice before BD surgery. *: FXRko-HFD vs. WT-HFD, $p < 0.05$. (B) Body weight changes in percentage in LFD-fed and HFD-fed WT and FXRko mice before BD surgery. FXRko-HFD vs. WT-HFD, $p < 0.05$ (n = 5 each group). (C) BD improves body weight (in grams) in both HFD-fed WT and FXRko mice (n = 5 each group). (D) BD improves body weight (in percentage) in both HFD-fed WT and FXRko mice. (E) BD improves fat mass

(epididymal white adipose tissue, eWAT in grams) in both HFD-fed WT and FXRko mice. WT-HFD vs. WT-BD, $p < 0.001$; and FXRko-HFD vs. FXRko-BD, $p < 0.001$. (F) BD improves fat mass (epididymal white adipose tissue, eWAT in percentage) in both HFD-fed WT and FXRko mice. (G) Liver weight in grams. Liver weight was significantly increased in LFD-fed and BD-treated FXRko mice. WT-LFD vs. FXRko-LFD $p < 0.01$; and WT-BD and FXRko-BD vs. WT-HFD and FXRko-HFD, $p < 0.05$, respectively. (H) The ratio of liver/body weight in percentage. WT-LFD vs. FXRko-LFD $p < 0.05$; and WT-BD and FXRko-BD vs. WT-HFD and FXRko-HFD, $p < 0.01$, respectively.

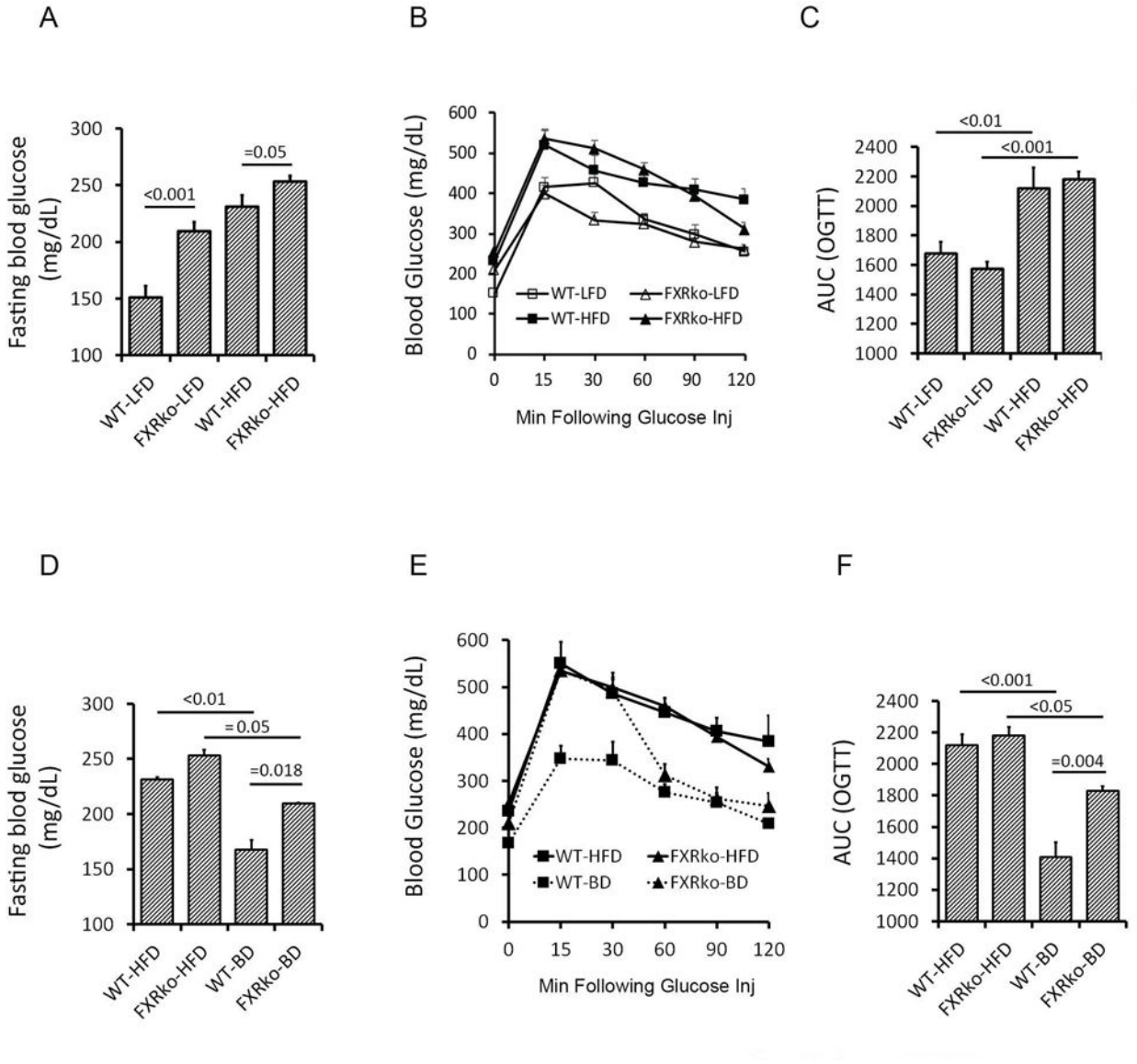

Figure 2.

BD improves hyperglycemia and glucose tolerance in WT mice, but not in FXRko mice (N = 5 each group). (A) LFD-fed FXRko mice develop hyperglycemia. Fasting blood glucose levels, WT-LFD vs. FXRko-LFD, $p < 0.001$; WT-HFD vs. FXRko-HFD, $p = 0.05$. (B) HFD impairs oral glucose tolerance (OGTT) in both WT and FXRko mice. (C) Areas under curve (AUC) of OGTT. (D) BD decreases fasting blood glucose levels in HFD-fed WT ($p < 0.01$) and in HFD-fed FXRko mice ($p = 0.05$). However, when WT-BD vs. FXRko-BD, $p = 0.018$. (E) BD improved glucose tolerance in HFD-fed WT and HFD-fed FXRko mice. (F) AUC of OGTT. WT-HFD vs. WT-BD, $p < 0.001$; FXRko-HFD vs. FXRko-BD, $p < 0.05$, and WT-BD vs. FXRko-BD, $p = 0.004$.

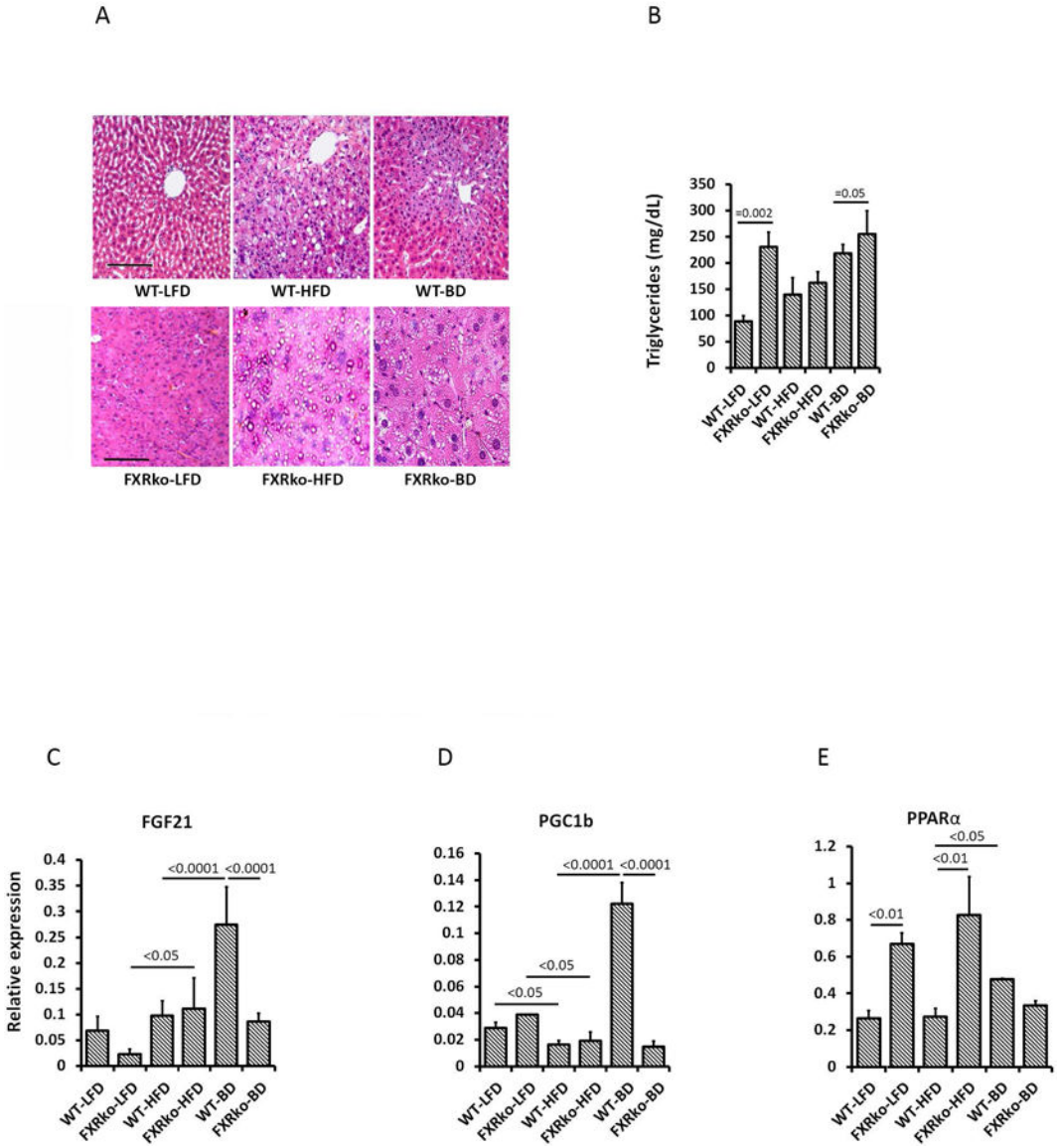

Figure 3.

Liver H&E staining, circulating triglyceride (TG) levels and hepatic gene expression. (A) BD improved HFD-induced liver steatosis in HFD-fed WT mice, but not in HFD-fed FXRko mice. (B) Circulating TG levels. FXRko-LFD vs. WT-LFD mice, $p = 0.002$; and WT-BD vs. FXRko-BD, $p = 0.05$. (C) Liver FGF21 gene expression. FXRko-LFD vs. FXRko-HFD, $p < 0.05$; and WT-HFD vs. WT-BD and WT-BD vs. FXRko-BD, $p < 0.0001$, respectively. (D) Liver PGC1ß expression. WT-HFD and FXRko-HFD vs. WT-LFD and FXRko-LFD, $p < 0.05$, respectively; WT-HFD vs. WT-BD and WT-BD vs. FXRko-BD, $p < 0.0001$, respectively. (E) Liver PPARα expression. WT-LFD vs. FXRko-LFD, $p < 0.01$; WT-HFD vs. FXRko-HFD, $p < 0.01$, and WT-HFD vs. WT-BD, $p < 0.05$.

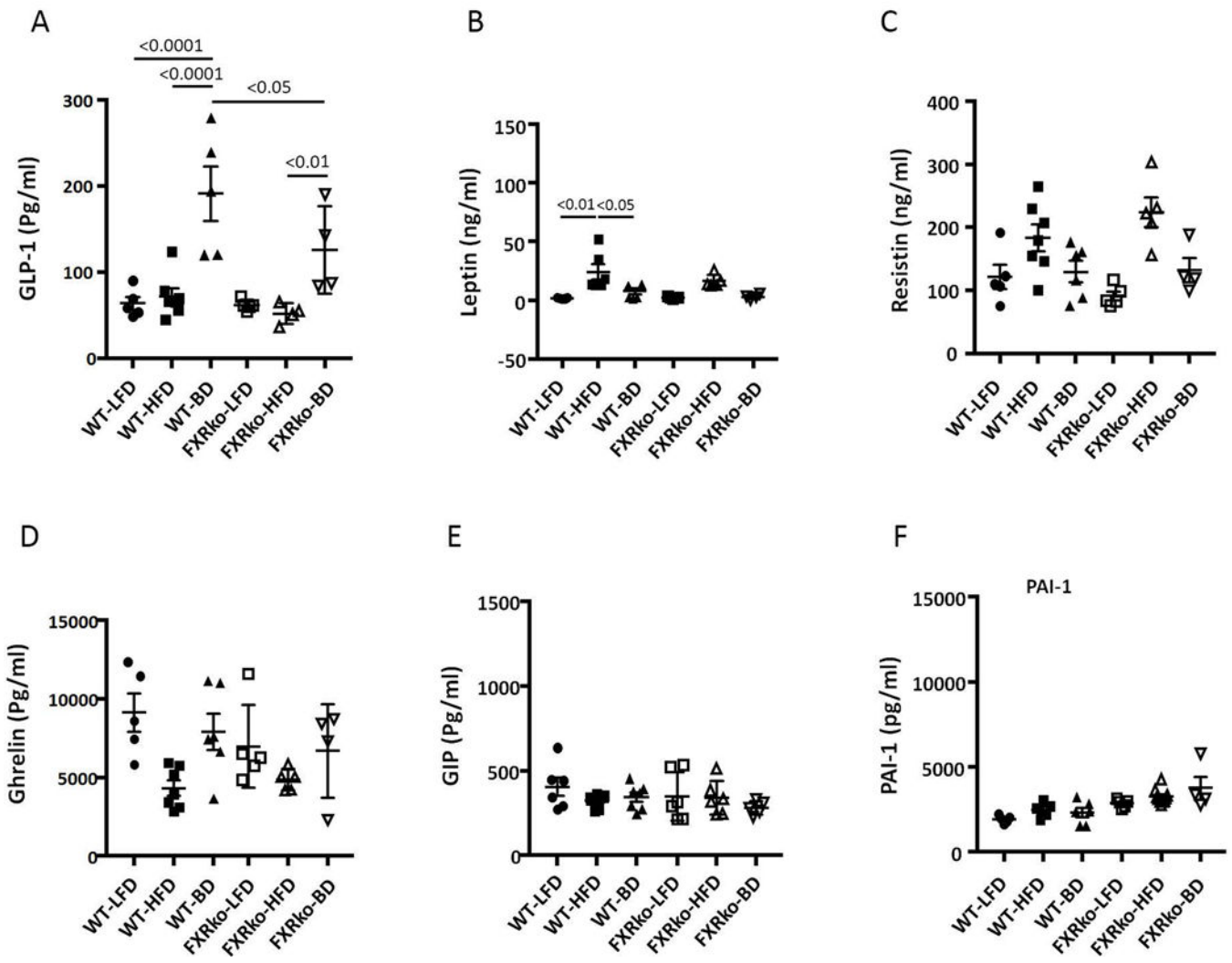

Figure 4.

Circulating endocrine hormones. (A) BD significantly increased circulating GLP-1. WT-BD vs. WT-LFD and WT-HFD, $p < 0.0001$; FXRko-HFD vs. FXRko-BD, $p < 0.05$, and WT-BD vs. FXRko-BD, $p < 0.05$. (B) HFD enhanced circulating leptin levels in HFD-fed WT mice, but not in HFD-fed FXRko mice. WT-LFD vs. WT-HFD, $p < 0.01$; and WT-HFD vs. WT-BD, $p < 0.05$. (C) BD decreased circulating resistin in both HFD-fed WT and FXRko mice, but not statistically significant ($p > 0.05$). (D) to (F), there were no statistical differences among groups ($p > 0.05$). N = 5 per group.

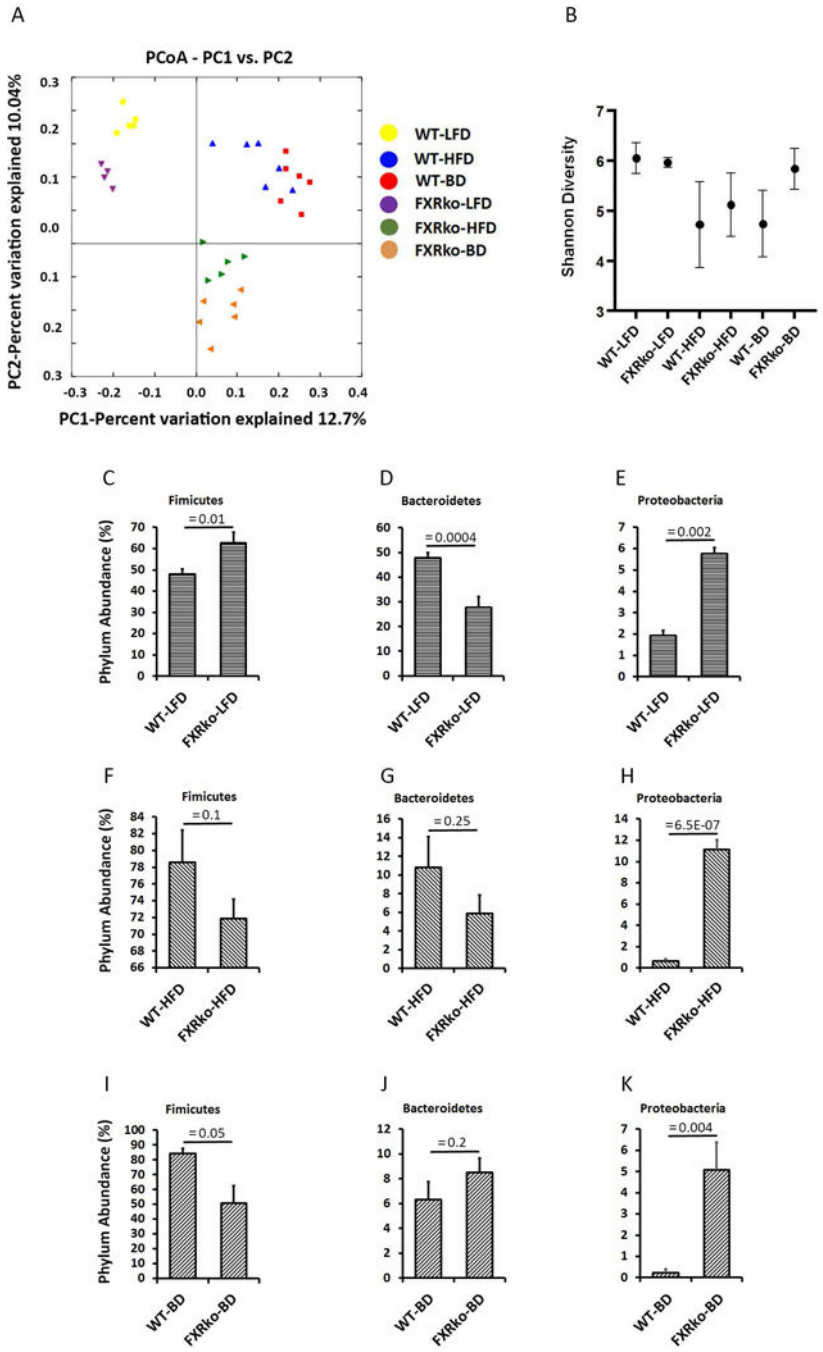

Figure 5.

The lack of FXR altered gut microbiota composition (N = 5 per group). (A) Weighted Unifrac analysis of beta diversity. (B) Shannon analysis of microbiome diversity. (C) Phylum Fimicutes in LFD-fed mice. WT-LFD vs. FXRko, $p = 0.01$. (D) Phylum Bacteroidetes in LFD-fed mice. WT-LFD vs. FXRko-LFD, $p = 0.0004$. (E) Phylum Proteobacteria in LFD-fed mice. WT-LFD vs. FXRko-LFD, $p = 0.002$. (F) Phylum Fimicutes in HFD-fed mice. WT-HFD vs. FXRko-HFD, $p = 0.1$. (G) Phylum Bacteroidetes in HFD-fed mice. WT-HFD vs. FXRko-HFD, $p = 0.25$. (H) Phylum Proteobacteria in HFD-

fed mice. WT-HFD vs. FXRko-HFD, $p = 6.5E-07$. (I) Phylum Fimicutes in BD-treated mice. WT-BD vs. FXRko-BD, $p = 0.05$. (J) Phylum Bacteroidetes in BD-treated mice. WT-BD vs. FXRko-BD, $p = 0.2$. (K) Phylum Proteobacteria in BD-treated mice. WT-BD vs. FXRko-BD, $p = 0.004$.

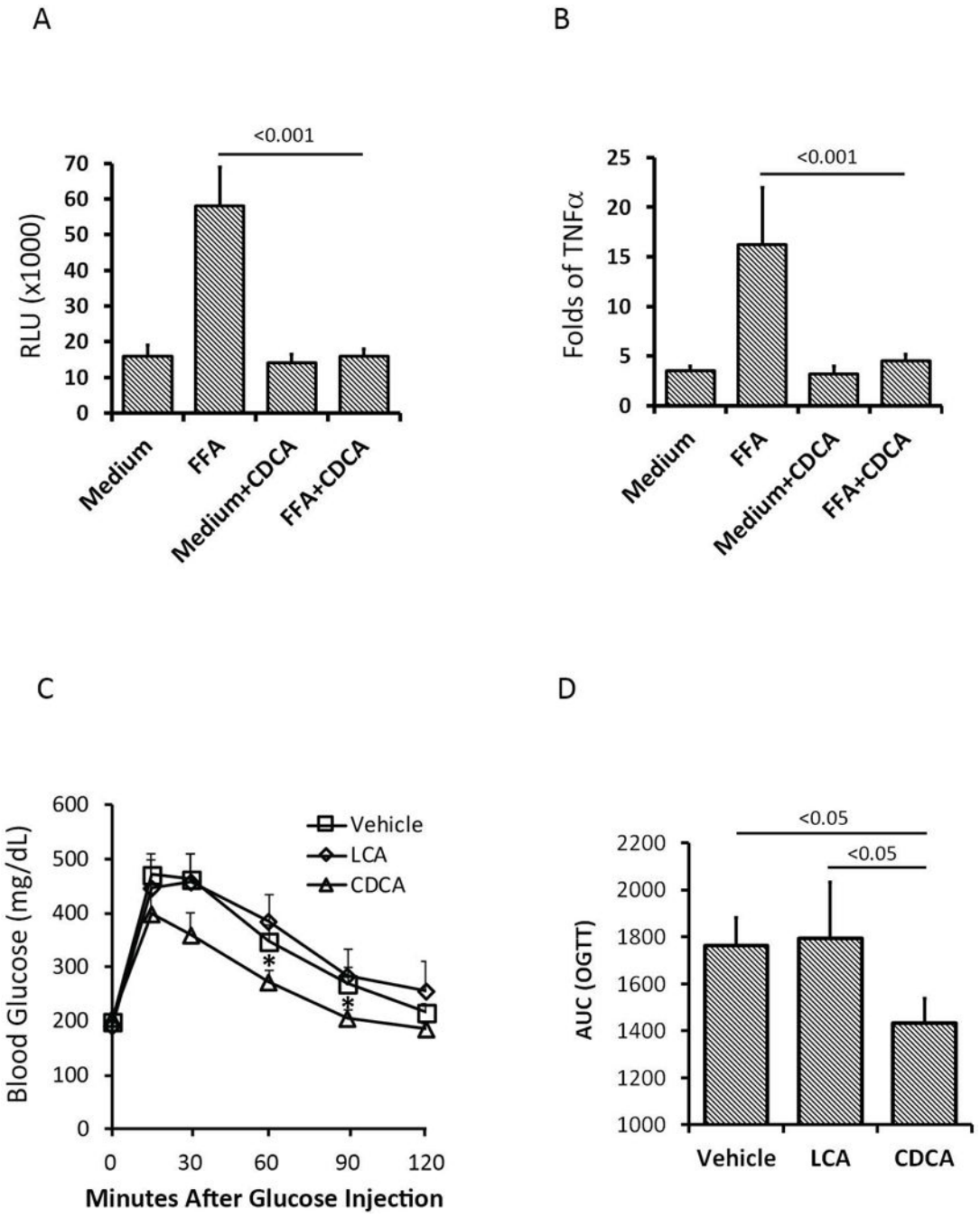

Figure 6.

FXR agonist CDCA inhibited inflammatory responses and improved glucose tolerance (N = 5 per group). (A) CDCA inhibited free fatty acid (FFA)-induced NF-B activity in bone marrow-derived macrophages (BMDM) culture. FFA+CDCA vs. FFA, $p < 0.001$. (B) CDCA inhibited TNFα expression in BKDK culture. FFA+CDCA vs. FFA, $p < 0.001$. (C-D) CDCA improved glucose tolerance in HFD-fed WT mice. CDCD vs. Vehicle and LCA, $p < 0.05$.